

MIXING CHARACTERISTICS OF ADDITIVES IN SLAG POT

Yannan WANG, Zhongfu CHENG, Bart BLANPAIN, Muxing GUO

KU Leuven, Department of Materials Engineering, 3001 Leuven, Belgium.

*yannan.wang@kuleuven.be, zhongfu.cheng@kuleuven.be,
bart.blanpain@kuleuven.be, muxing.guo@kuleuven.be.*

Introduction

Approximately 10 million tons of Basic Oxygen Furnace (BOF) slag are produced annually in Europe.¹ The BOF slag is conventionally disposed through landfilling/dumping, leading to land occupation, environmental impact and waste of material resource.² In order to solve these problems, considerable efforts to reuse BOF slag have been made in the last decades.³ However, the application of BOF slag is restricted by its volume expansion due to the presence of free lime.⁴ For the purpose of stabilising BOF slag through modifying the slag chemistry for high-added value products, silica-rich additives/slag modifiers are injected into the molten BOF slag with oxygen or nitrogen as carrier gas.⁵ Therefore, the study of mixing characteristics of additives in molten BOF slag is of significant importance for process control and optimisation.

It is very difficult to perform lab experiments to understand the mixing behaviour of slag modifier in a slag pot. Therefore, a modelling approach is very beneficial for a parametric study. In the present work, the Volume of Fluids (VOF) model is used for the gas-liquid two-phase flow and the Discrete Phase Model (DPM) is employed to track the particle migration. In order to simplify the simulation, the volume fraction of the solid additives is considered dilute.

The objective of this paper is to develop a 3D numerical approach to study the migration of the solid additives, which can help industrial operators to understand the effect of the operational factors, *e.g.*, lance depth and gas flow rate, on the mixing behaviour of the additives, and therefore to optimise the process.

Numerical methodology

VOF model

In the VOF model the variables and properties are shared by all phases and represent volume-averaged values. Because of this, there is only one set of continuity and momentum equations, which are listed as follows:

$$\frac{\partial}{\partial t}(\alpha_g \rho_g) + \nabla \cdot (\alpha_g \rho_g \vec{u}_g) = 0 \quad (1)$$

$$\frac{\partial}{\partial t}(\rho \vec{u}) + \nabla \cdot (\rho \vec{u} \vec{u}) = -\nabla p + \nabla \cdot \bar{\tau} + \rho \vec{g} + \vec{F}_{csf} + \vec{F}_{int} \quad (2)$$

$$\alpha_l = 1 - \alpha_g \quad (3)$$

where g , α_g , α_l , ρ , u , $\bar{\tau}$, p , g , \vec{F}_{csf} and \vec{F}_{int} represent the gas phase, gas volume fraction, slag volume fraction, density, velocity, stress tensor, pressure, gravity acceleration and surface tension force, respectively. The flow turbulence is simulated by the Large Eddy Simulation with the dynamic Smagorinsky-Lilly model.^{6,7}

DPM model

The solid additives are tracked by solving Newton's second law. The dissolution of the additives is not considered in this work. Hence, the interaction between the solid particle and molten slag is physically interpreted through the momentum exchange due to interphase forces, *e.g.*, drag force, virtual mass force and lift force. The mathematical expression of the particle migration is given in Equations (4) and (5).

$$m \frac{d\vec{v}}{dt} = \vec{F}_D + \vec{F}_{VM} + \vec{F}_L \quad (4)$$

$$\frac{dx}{dt} = \vec{v} \quad (5)$$

where m , \vec{v} , \vec{F}_D , \vec{F}_{VM} and \vec{F}_L indicate the particle mass, particle velocity, drag force, virtual mass force, lift force, respectively.

Numerical setup

The simulations are performed using the commercial software package ANSYS FLUENT 16.2. The geometrical information, operational parameters and materials properties used in the simulation are shown in Table 1. The velocity inlet and pressure outlet are used for the simulation. The Pressure-Implicit with Splitting of Operators scheme (PISO)⁸ is adopted for the solution of the velocity-pressure coupling equation. The PREssure STaggering Option (PRESTO!) and second order upwind are used as the spatial discretisation scheme for the pressure and momentum equations, respectively. In this study, the convergence criterion is 1×10^{-6} . The time step is 1×10^{-4} s.

Table 1: Geometrical dimensions, operational parameters and material properties

Top diameter of the slag pot, m	3.36
Bottom diameter of the slag pot, m	2.39
Height of the slag pot, m	3.558
Lance diameter, m	0.04
Height of slag level, m	3.0
Submerged depth of lance L , m	0.3, 1.0
Gas flow rate Q , Nm ³ /h	100, 170
Pressure, kPa	300
Density of slag, kg/m ³	3000
Viscosity of slag, kg·m ⁻¹ ·s ⁻¹	0.1
Density of gas, kg/m ³	0.574
Viscosity of gas, kg·m ⁻¹ ·s ⁻¹	5.87×10^{-5}
Interfacial tension of slag/air, N/m	0.55
Solid additive size, m	0.002

Results and discussion

Figure 1 shows that the particle migration varies with the lance depth in slag pot. At time = 50 s, the mixing zone at the lance depth of 1.0 m (Figure 1b) is much larger than that at the lance depth of 0.3 m (Figure 1a), as indicated by the particles occupied region (red colour). Clearly, there is almost no dead zone when the lance depth is 1.0 m, while a large dead zone exists at the bottom of the slag pot when the lance depth is 0.3 m. Apparently, increasing lance depth can increase the mixing zone, leading to a better mixing of the slag modifier.

Particle distribution in slag pot as a function of the gas flowrate is shown in Figure 2. Increasing the gas flowrate enlarges the mixing zone. This is because the initial kinetic energy of the injected particle is increased as gas flowrate increases. Therefore, a larger gas flowrate is needed for a better additives mixing.

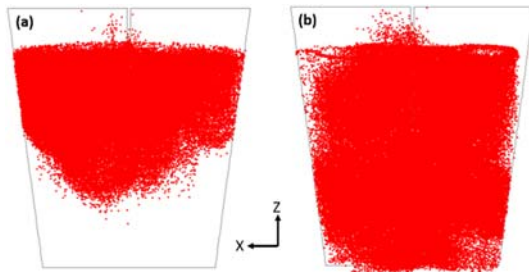


Figure 1: Particle distribution at (a) $L = 0.3$ m and (b) $L = 1.0$ m at 50 s ($Q = 170$ Nm³/h) (X-Z median plane of a 3D model)

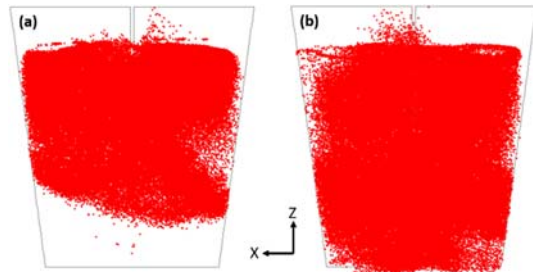


Figure 2: Particle distribution at (a) $Q = 100$ Nm³/h and (b) $Q = 170$ Nm³/h at 50 s ($L = 1.0$ m) (X-Z median plane of a 3D model)

The mixing zone under different operational conditions can be easily inspected by the particle distribution. However, it is difficult for this method to obtain a quantification of the mixing time, because the present method does not take the additive dissolution into account and therefore species diffusion is not considered. Nonetheless, a semi-quantitative mixing time can be obtained, and the mixing time of the above cases is listed in Table 2. The mixing time of Case II is approximately 50 s, decreasing by 76.2% compared to 210 s of Case I. The mixing time of Case III, 140 s, is around 2.8 times larger than that of Case II. Therefore, increasing the lance depth and the gas flow rate can significantly reduce the mixing time.

Table 2: Mixing time under different operational conditions

Case	Mixing time, s
I: $L = 0.3 \text{ m}$, $Q = 170 \text{ Nm}^3/\text{h}$	210
II: $L = 1.0 \text{ m}$, $Q = 170 \text{ Nm}^3/\text{h}$	50
III: $L = 1.0 \text{ m}$, $Q = 100 \text{ Nm}^3/\text{h}$	140

Conclusions

Three-dimensional VOF+DPM numerical simulations have been performed to study the mixing behaviour of the solid particles in molten BOF slag. The model is able to track the additives migration. The numerical results suggest that increasing lance depth and gas flowrate can significantly improve mixing of the solid additives in the slag pot. Further simulations are needed to optimise the operational conditions for a better mixing.

References

1. Euroslag, <https://www.euroslag.com/wp-content/uploads/2019/01/Statistics-2016.pdf>.
2. H. Shen, E. Forssberg, "An Overview of Recovery of Metals from Slag", *Waste Manage*, **23** (10) 933-49 (2003).
3. H. Yi, G. Xu, H. Cheng, J. Wang, Y. Wan, H. Chen, "An Overview of Utilization of Steel Slag", *Procedia Environ Sci*, **16** 791-801 (2012).
4. G. Wang, Y. Wang, Z. Gao, "Use of Steel Slag as A Granular Material: Volume Expansion Prediction and Usability Criteria", *J Hazard Mater*, **184** (1-3) 555-60 (2010).
5. D. Durinck, F. Engström, S. Arnout, J. Heulens, P.T. Jones, B. Björkman, B. Blanpain, P. Wollants, "Hot Stage Processing of Metallurgical Slags", *Resour Conser Recy*, **52** (10) 1121-1131 (2008).
6. M. Germano, U. Piomelli, P. Moin, W.H. Cabot, "A Dynamic Subgrid-scale Eddy Viscosity Model", *Phys Fluids A*, **3** (7) 1760-65 (1991).
7. D.K. Lilly, "A Proposed Modification of the Germano Subgrid-scale Closure Method", *Phys Fluids A*, **4** (3) 633-35 (1992).
8. R.I. Issa, "Solution of the Implicitly Discretised Fluid Flow Equations by Operator-splitting", *J Comput Phys*, **62** (1) 40-65 (1986).